

Review:

# On-Chip FRET Graphene Aptasensor

Yuko Ueno<sup>\*,†</sup> and Kazuaki Furukawa<sup>\*\*</sup>

\*NTT Basic Research Laboratories, NTT Corporation  
3-1 Morinosato, Wakamiya, Atsugi, Kanagawa 243-0198, Japan

†Corresponding author, E-mail: ueno.yuko@lab.ntt.co.jp

\*\*Meisei University, Tokyo, Japan

[Received May 23, 2017; accepted November 23, 2017]

We review the recent advances in the use of our originally developed on-chip graphene aptasensor to detect biologically important proteins, such as cancer markers. The detection mechanism, based on fluorescence resonance energy transfer (FRET), occurs at a graphene–biomolecule interface. In our system, the graphene surface is modified with a pyrene–aptamer–dye probe. Pyrene functions as a linker to the graphene surface, the aptamer as a probe for selective protein recognition, and the dye as a fluorescence detection tag. Here, graphene behaves simultaneously as both an efficient acceptor for FRET over the entire visible region and as a strong adsorbate for single-stranded DNA (ssDNA), such as aptamers, via  $\pi$ - $\pi$  interactions in the  $sp^2$  domain. The system allows us to perform molecular detection on a solid surface, which is advantageous for realizing on-chip sensors. Such on-chip sensors allow parallel analysis systems, such as array sensors. This enables the quantitative comparison of different samples by forming a multi-channel configuration and/or a micropattern with different probes. Moreover, detecting the target protein is possible simply by adding a sample of less than 1  $\mu$ L to the on-chip sensor; detection is completed in approximately 1 min. Aptasensors can be used for the detection of many different targets simply by replacing the aptamers. The simultaneous detection of multiple target molecules on a single chip using a  $2 \times 3$  linear-array aptasensor was demonstrated here. Improved sensitivity was observed when a DNA spacer was incorporated into the aptamer, demonstrating that the probe can be modified in interesting ways.

**Keywords:** graphene, aptamer, biosensor, microchannel, fluorescence resonance energy transfer

## 1. Introduction

Graphene is an atomically thin two-dimensional sheet consisting of a hexagonal honeycomb lattice of carbon atoms. It has attracted significant attention for its unique properties, including extremely high mechanical strength, thermal conductivity, electronic mobility, and thermal and chemical stability [1]. Graphene was isolated in 2004 by Profs. Geim and Novoselov of the University of Manch-

ester, who won the 2010 Nobel Prize in Physics for their work. The mass production of graphene, difficult at that time, has progressed greatly. Now, monolayer graphene measuring several tens of square centimeters can be obtained using synthetic techniques typified by the chemical vapor deposition (CVD) process [2].

Graphene oxide (GO), the most widely utilized chemical derivative of graphene, has also attracted considerable interest [3, 4]. GO is an oxidized form of graphene with an atomically thin sheet-like structure, which contains nanometer-sized graphene-like  $sp^2$  domains. In GO, many CC bonds in the graphene sheet are broken and linked with oxygen, forming carbon-oxygen bonds. GO is prepared very differently from graphene; its mass production is also relatively easy. We can chemically synthesize GO by oxidizing graphite powder in a strong acid. This yields a large quantity of GO; however, it is difficult to obtain synthesized GO larger than 1 mm<sup>2</sup>. GO is unsuitable as a replacement for graphene in electronic materials that require high charge mobility, but can be used in optical devices and as a sensing material [5, 6].

On the surface of graphene (or the  $sp^2$  domains in GO), energy transfer occurs when molecules are located near the surface. The energy transfer yield depends on the degree of molecular interaction between the adsorbed molecules and the graphene surface. For example, graphene works as an excellent acceptor for fluorescence resonance energy transfer (FRET) over the entire visible wavelength region [7]. Thus, when a fluorescent molecule such as a dye is located very near the graphene surface, the fluorescence is quenched. By exploiting the energy transfer properties of graphene, we can visualize biological and chemical reactions by converting these invisible molecular behaviors into measurable physical quantities, such as light and electricity. This makes graphene a promising material for unique biosensors. By employing this concept, early studies on DNA sensors and aptasensors have been conducted on aqueous dispersions of GO [8].

In contrast, we have proposed and developed a molecular detection system that works on graphene or GO supported on a solid surface. In this study, we introduce our original design for a graphene-based aptasensor that enables the selective and quantitative detection of biologically important proteins, such as cancer markers.



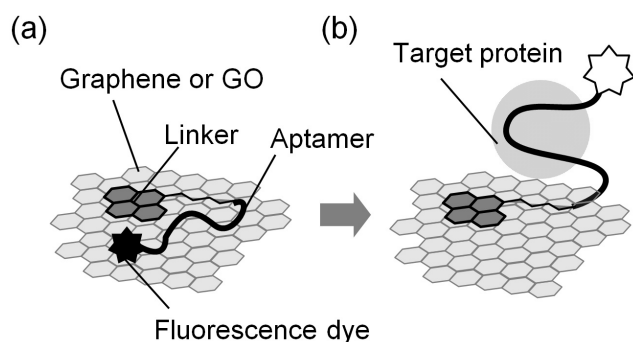


**Fig. 1.** Design of protein detection system built on graphene-biomolecule interface, (a) without target protein and (b) with target protein.

## 2. Mechanism of Graphene Aptasensor

Our graphene aptasensor uses a graphene–biomolecule interface, here indicating a solid surface functionalized with biological molecules, modified with an aptamer. One end of the aptamer is labeled with a fluorescent dye and the other end is connected to a pyrene linker molecule, which shows a strong affinity to graphene (or the  $sp^2$  domains of GO). Thus, the aptamer is firmly fixed to the graphene surface. The detection process of the graphene aptasensor occurs as follows. Initially, the dye-conjugated aptamer is adsorbed on the graphene surface via physical adsorption ( $\pi$ - $\pi$  interactions), and thus the dye is located near the graphene surface. Here, the fluorescence of the dye is quenched by graphene via FRET and is thus barely observable (**Fig. 1(a)**). If the target of the aptamer is present in the system, the aptamer forms a complex with the target and leaves the graphene surface. This then lifts the dye molecule from the graphene surface and the fluorescence is recovered (**Fig. 1(b)**). We detect the target molecule by observing the fluorescence [9].

Aptamers have a wide variety of targets and many advantages as molecular recognition probes [10]. Aptasensors are versatile because they can be used in the detection of many different targets by replacing the aptamers. We confirmed the versatility of our on-chip graphene aptasensor simply by changing the aptamers but retaining the same sensor composition (see section 6). Moreover, aptamers can be flexibly designed without loss of bioactivity. Thus, we can design and construct various biomolecular probes by conjugating additional functions with aptamers (see section 9). Lastly, aptamers are chemically stable. We confirmed that aptasensors stored at a normal temperature and pressure for more than a month operated normally, as if newly made.

## 3. Protein Detection on the Surface of a Single GO Piece Fixed on a Solid Support

At the start of this study, we realized biomolecular interfaces by using easily available GO and confirmed the usefulness of aptasensors for protein detection. Our

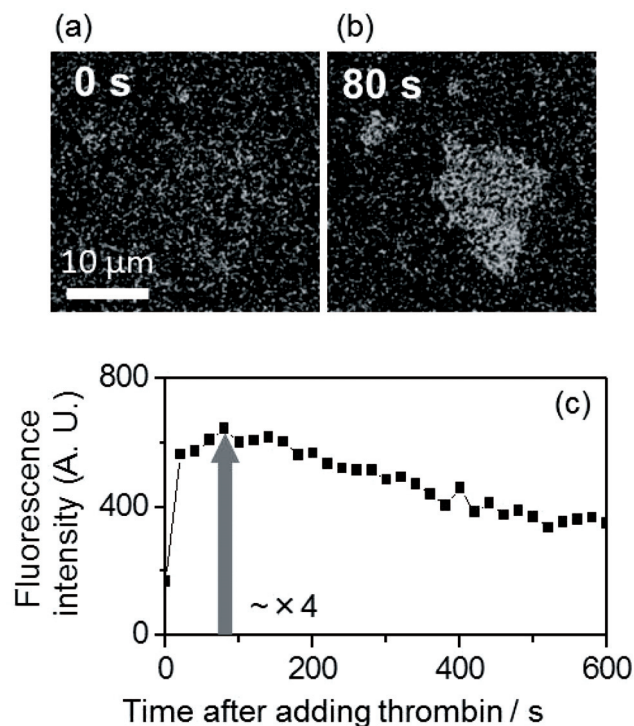


**Fig. 2.** LSM images of a specific GO piece (a) before thrombin addition and (b) 80 s after thrombin addition. (c) A plot of fluorescence intensity vs. time after thrombin addition.

sensing system is distinctive in allowing us to undertake molecular detection on a solid surface. The first advantage of this point is that we can use several surface characterization methods to analyze the phenomena occurring locally at the biomolecular interfaces during molecular detection. We performed the direct observation of protein detection on the surface of a single GO piece fixed on a solid support by using a confocal laser scanning microscope (LSM) and an atomic force microscope (AFM). We used thrombin, an important protein for blood clotting, as the detection target in this study [9].

**Figures 2(a)** and **(b)** show the fluorescence microscope images of GO before and after thrombin addition, respectively. The image is dark before the addition; it becomes brightly fluorescent after the addition. This is attributed to the fluorescence from the dye at the aptamer terminus. The time-lapse observations of the green fluorescence revealed that the fluorescence intensities reached approximately four times higher than the background fluorescence levels, and thus showed that the increase was significant enough for the detection of the target proteins (**Fig. 2(c)**). Since the images were collected by a confocal microscope detecting fluorescence only at the focused plane, it is clear that the green fluorescence originated from the complex formation between the thrombin aptamer and thrombin on the GO surface.

Next, we observed the GO surface using AFM to estimate the adsorption amount of thrombin. By observing the same piece of GO using LSM and AFM, we eliminated individual and environmental differences between GO flakes. **Fig. 3** shows the AFM topographies before

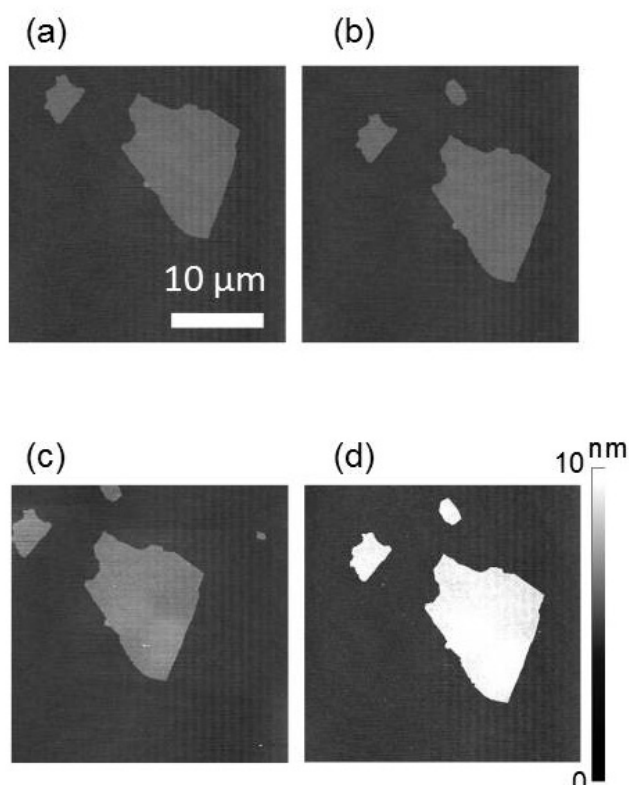
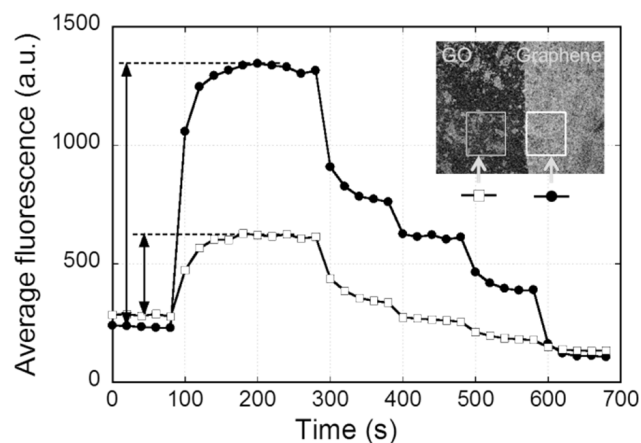


**Fig. 3.** AFM topographies of the GO piece in **Fig. 2** observed (a) before chemical modifications, (b) after modification by linker, (c) after modification by thrombin aptamer, and (d) after thrombin addition. All the images were obtained under atmospheric conditions.

and after thrombin detection. The shape of the piece corresponds to that of the green fluorescence in **Fig. 2**, which is sufficient proof that we observe the same piece of GO. The average thickness of the GO is changed from (a) 1.11 nm, (b) 1.16 nm, and (c) 1.73 nm to (d) 4.62 nm. The obvious increase of  $\sim 2.9$  nm in the thickness is due to the thrombin adsorption. The size of thrombin is about 4 nm in diameter in solution conditions. The increase in thickness is smaller than this molecular size, suggesting that thrombin does not fully cover the GO surface. In addition, the AFM topographies were observed in dry atmospheric conditions, which may cause the transformation and shrinkage of thrombin. Thus, the observed thicknesses in **Fig. 3** may not be quantitatively accurate. However, the comparison of thicknesses in the same conditions using the same GO single piece is clearly significant. Another important feature in **Fig. 3** is that no thrombin is observed on the hydrophilic  $\text{SiO}_2$  surface supporting the GO piece. Although proteins like thrombin often adsorb on many kinds of surfaces, adsorption is suppressed in our system. The selectivity of thrombin adsorption could not be determined without the AFM observations.

#### 4. Aptasensor Built on Continuous Single-Layer Graphene Surface

In our GO aptasensor, we used a pyrene linker that showed a strong affinity with the graphene-like domains



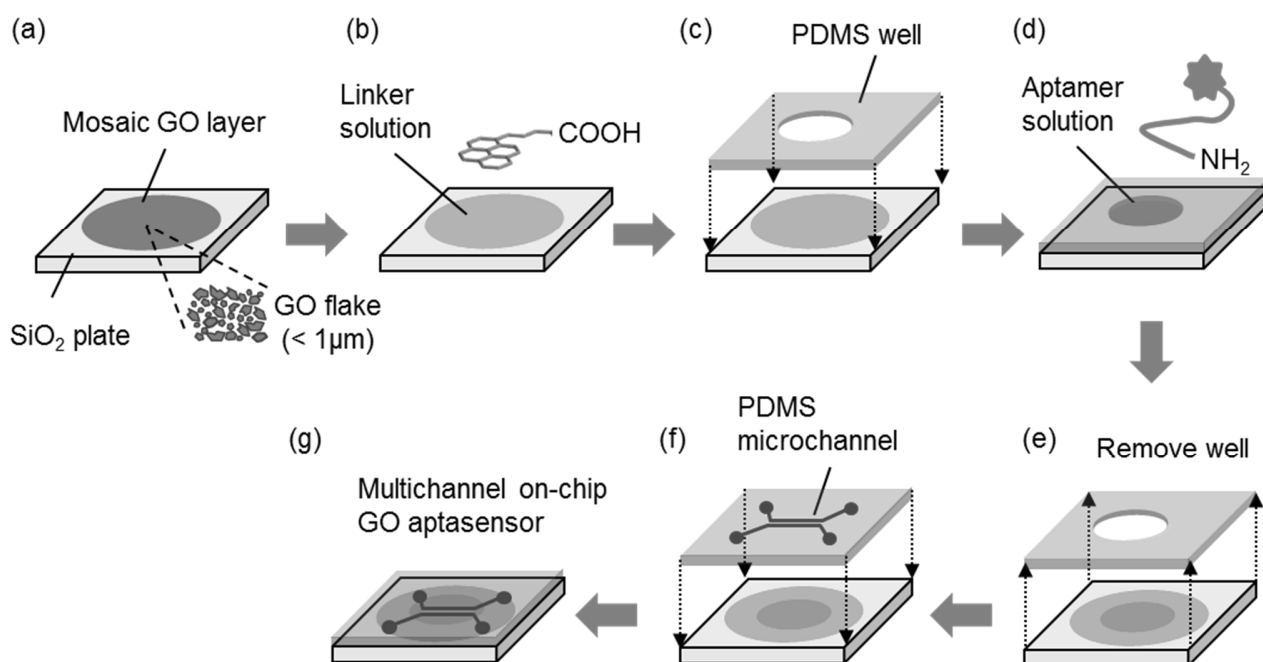
Source: ACS Sensors Vol.1 No.6 [9]

**Fig. 4.** Quantitative comparison of PSA detection performance of graphene and GO sensors.

to immobilize the aptamer. However, the surface area of the graphene-like domain reached 50% maximum of a GO flake. By changing the platform from GO to graphene, we could realize a solid surface with a 100% graphene structure. The second advantage of our system for molecular detection on a solid surface is that we can use either water-dispersive GO or hydrophobic graphene as the sensor platform [11].

We prepared an aptasensor on a commercially available single-layer graphene surface fixed on a solid substrate. Here we used prostate-specific antigen (PSA, the most common serum marker for diagnosing prostate cancer) as the target molecule. We confirmed that the substrate was almost fully covered with a single layer of graphene by observing optical and Raman spectral images before measuring the sensing performance. The fluorescence intensity was initially small and increased steeply after PSA was added. The fluorescence intensity was almost homogeneous across the observed area of more than  $100 \mu\text{m} \times 100 \mu\text{m}$ . Next, we compared the protein detection performance quantitatively by using graphene and GO biosensors prepared on the same chip. We fixed graphene and GO on the  $\text{SiO}_2$  surface of a solid substrate and modified both surfaces with a dye-labeled aptamer under the same conditions. We observed increases in the fluorescence intensity on both the graphene and GO surfaces on the addition of PSA ( $33 \mu\text{g/mL}$  @  $t = 100$  s) (**Fig. 4**).

After performing several observations under conditions of constant PSA concentration, we added deionized (DI) water to dilute the PSA solution. The fluorescence intensities became weaker as the concentration of the PSA solution decreased ( $20, 14, 11,$  and  $9 \mu\text{g/mL}$  @  $t = 300$  s,  $400$  s,  $500$  s, and  $600$  s). We thus demonstrated the successful operation of the sensor on both graphene and GO surfaces. We compared the performance of the graphene sensor with that of the GO sensor by using the average fluorescence intensities before PSA addition and the maximum fluorescence intensity ratios from after PSA detection. The graphene sensor yielded a larger intensity than GO, with a ratio exceeding 3. We conclude that



Source: Anal. Chim. Acta Vol.866 (25 March 2015) [10]

Fig. 5. Multichannel on-chip GO aptasensor preparation procedure.

the graphene is superior to GO in terms of building a biomolecular interface for fluorescence-based sensors.

## 5. On-Chip Aptasensor by Using Microchannel Configuration for Quantitative Detection

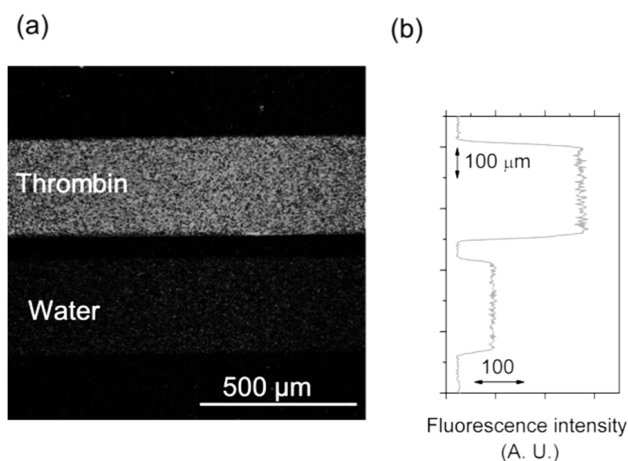
The third advantage of our system is that we can realize an on-chip sensor by combining the graphene–biomolecule interface with a microfluidic device. Briefly, we fabricated an on-chip graphene aptasensor by placing a polydimethylsiloxane (PDMS) sheet with microchannels on a solid substrate, and formed the graphene aptasensor on the PDMS surface. We can fabricate a microchannel with the desired design by using photolithographic techniques. The number of the channels is also controllable. Thus, if we form multiple microchannels on a single chip, we can perform a high-throughput analysis by parallelizing several different measurements. Moreover, if we use one of the multiple channels as an internal standard, eliminating the effect of fluorescence degradation caused by laser exposure and other noise, we realize a consistent reference-to-sample comparison for accurate quantitative analysis [12].

The PDMS microchannel requires no external power or expensive equipment to drive liquid flow, since the flow in the microchannel is driven by capillary force [13]. Thus, detecting the target protein is possible simply by adding a sample smaller than  $1\ \mu\text{L}$  to the on-chip sensor and simultaneously measuring the fluorescence emitted from the graphene surfaces located in each microchannel. The reaction to form the aptamer–protein complex is completed in approximately 1 min. Real-time detection is

possible by tracking the fluorescence intensity of the microchannels by adding different sample solutions sequentially (See section 8). For comparison, ELISA enzyme-linked immunosorbent assay is one of the most popular protein detection methods. A commercially obtained ELISA kit requires the sample volume and assay time of at least  $100\ \mu\text{L}$  and 3 h, respectively.

Figure 5 illustrates the multichannel on-chip GO aptasensor preparation procedure. The GO dispersion is spin-coated on a hydrophilic surface consisting of an  $18 \times 18\ \text{mm}$  glass plate treated with  $\text{O}_2$  plasma prior to the GO coating (Fig. 5(a)). The size of the GO pieces and the concentration of the GO dispersion for this procedure are described in detail in the results and discussion section, together with the sensing performance. The GO pieces are then covered with a drop of a 5 mM DMF solution of the linker (1-pyrenebutanoic acid-succinimidyl ester) for 1 h (b), rinsed with DMF, and then dried in a  $\text{N}_2$  stream. A PDMS sheet with a hole in it is placed on the plate to form a well (c) and  $3.5\ \mu\text{L}$  of aptamer solution is poured into the well to cover the GO surface for 1 h (d). The amine group at the 3'-terminus of the aptamer is bonded to the pyrene linker by a dehydration reaction; thus, the aptamer is immobilized on the GO surface. The PDMS well is removed from the plate and the plate is rinsed with DI water (RNase-free distilled water used for the RNA aptamer) to remove unreacted aptamer, and then dried in a  $\text{N}_2$  stream (e). Another PDMS sheet with multiple microchannels is mounted on the glass plate (f). The multichannel on-chip GO aptasensor is then ready for detection (g). All the above procedures are performed at room temperature.

We prepared the graphene aptasensor by using the same procedure, except for Fig. 5(a). We replaced the proce-



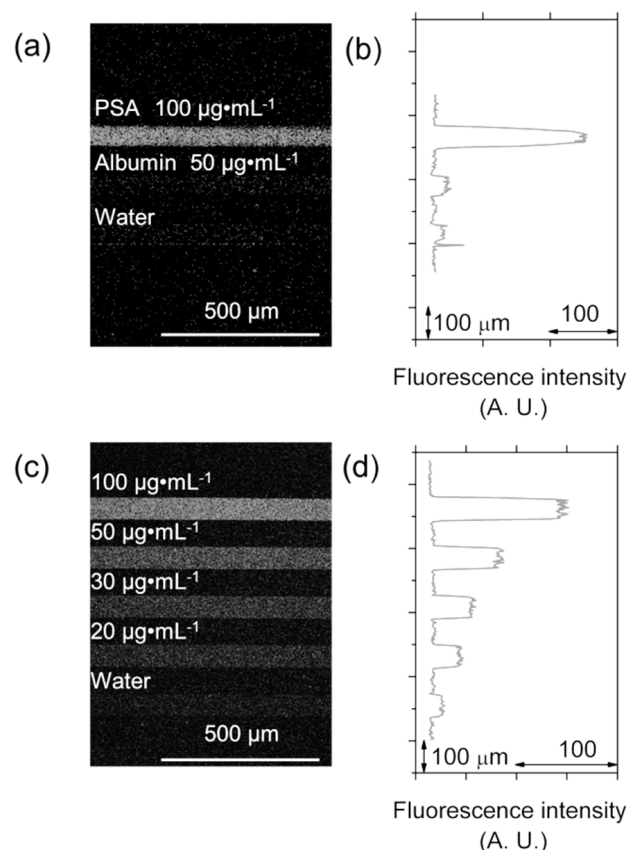
Source: Anal. Chim. Acta Vol.866 (25 March 2015) [10]

**Fig. 6.** (a) Fluorescence image of the on-chip aptasensor after injecting thrombin solution ( $100 \mu\text{g}\cdot\text{mL}^{-1}$ ) and DI water into the top and bottom channels and (b) the line profile of the fluorescence intensity.

procedure shown in **Fig. 5(a)** as follows. A CVD-grown sample of graphene on copper foil was cut into a piece of the required size. The graphene surface was covered with poly (methyl methacrylate) (PMMA) by spin-coating. The piece was floated on  $\text{FeCl}_3$  solution (3N) for  $\sim 2$  h to etch the copper. The  $\text{FeCl}_3$  was replaced with DI water to wash the bottom surface of the graphene with a PMMA top layer. The graphene floating on water was then transferred onto the glass substrate. The PMMA film was removed in hot acetone.

**Figure 6(a)** shows the fluorescence image of the GO aptasensor for thrombin detection, on which a dual microchannel is mounted. The fluorescence in the top channel, filled with the thrombin solution, is much brighter than that in the bottom channel, which contains DI water. **Fig. 6(b)** shows the line profile of the fluorescence intensity, which has an average of  $\sim 480$  pixel data along the horizontal axis for the detection of  $100 \mu\text{g}\cdot\text{mL}^{-1}$  thrombin solution. The signal, an output of the detector of the LSM (photomultiplier tube), is almost constant in the channel along the vertical axis. The results show that the mosaic GO layer in the microchannel is formed almost homogeneously on a scale larger than  $1 \text{ mm} \times 1 \text{ mm}$ . The ratio of the fluorescence intensity of the sample channel to that of the reference channel reaches approximately 4:1.

Next, we examined the selectivity of this sensor for the detection of PSA. Here we prepared the aptasensor with a triple-microchannel configuration. We measure the fluorescence images when PSA, human albumin solution, and DI water are injected into the top, middle, and bottom channels, respectively (**Fig. 7(a)**). Albumin, the most abundant protein in human blood plasma, causes no change in the fluorescence intensity, in the same way as DI water (**Fig. 7(b)**). This proves the selectivity of our aptasensor for PSA detection. We also examine the dependence of the fluorescence intensity on the PSA concentration. We used a quintuple-microchannel configura-



Source: Anal. Chim. Acta Vol.866 (25 March 2015) [10]

**Fig. 7.** (a) Fluorescence images of the aptasensors after injecting PSA solution, human albumin solution, and DI water into the top, middle, and bottom channels obtained in an area including all three microchannels, (c) after injecting different concentrations of PSA solution into each channel obtained in an area including all five microchannels, and (b, d) the line profiles of their fluorescence intensities.

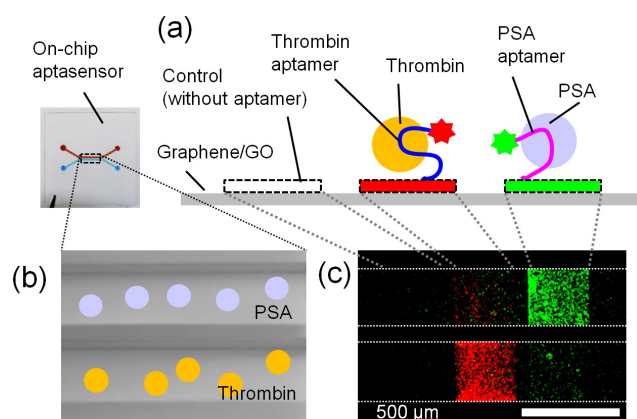
**Table 1.** Aptamers and their targets.

| Aptamer sequence               | Target   | Type |      |
|--------------------------------|----------|------|------|
| 5'-GGTTGGTGTGGTTGG-3'          | Thrombin | DNA  | [14] |
| 5'-ATTAAAGCTCGCCATCAAA TAGC-3' | PSA      | DNA  | [15] |
| 5'-GUCGGCAUGC GGUA-3'          | HA       | RNA  | [16] |

tion and injected PSA solution of four different concentrations and DI water as a reference into the microchannels (**Figs. 7(c), (d)**). The results show that the fluorescence intensity weakens as the PSA concentration is decreased. The above observations cannot be achieved without the multichannel on-chip graphene/GO aptasensor.

## 6. Versatility of Graphene Aptasensor

In general, aptasensors are versatile because they can be used for the detection of many different targets by replacing the aptamers. However, the versatility of an aptamer immobilized on a solid surface at a terminus has not yet been confirmed. We confirmed that several DNA and



Source: Anal. Chim. Acta Vol.866 (25 March 2015) [10]

**Fig. 8.** (a) Layout of a linear-array GO aptasensor, (b) image of microchannel, and (c) color-composite fluorescence image of GO aptasensor after injecting PSA solution and thrombin solution into the top and bottom channels.

RNA aptamers, shown in **Table 1**, are sufficiently active to realize on-chip graphene/GO aptasensors through the detection of corresponding target proteins. The versatility of the on-chip graphene/GO aptasensors was successfully demonstrated simply by changing the aptamers but retaining the same sensor composition [12].

## 7. A Linear-Array Sensor for Simultaneous Multiple Protein Detection

We fabricated a  $2 \times 3$  linear-array aptasensor by using two different aptamers for different targets, namely thrombin and PSA. We label these with red fluorescent TAMRA and green fluorescent FAM, respectively, for ease of distinction (**Fig. 8(a)**). After injecting PSA and thrombin solution into the top and bottom microchannels, respectively (**Fig. 8(b)**), we obtain a color-composite fluorescence image of the sensor (**Fig. 8(c)**). The red and green fluorescence images were observed simultaneously by using two different filters with the same excitation light source. A large amount of FAM fluorescence is observed at the PSA aptamer position in the upper channel, whereas little fluorescence is observed in other areas, including the control area. In the same manner, a large TAMRA fluorescence is observed at the thrombin aptamer position in the lower channel. Little fluorescence is observed in other areas. Although cross-reactions are observed, the signals are small enough to distinguish from the target reactions. Thus, a simultaneous multiple-protein detection system on a single chip was successfully demonstrated [12].

## 8. Real-Time Protein Detection

We also demonstrated real-time protein detection by using an on-chip aptasensor under solution flow conditions. Here, we used PSA as the target molecule. During

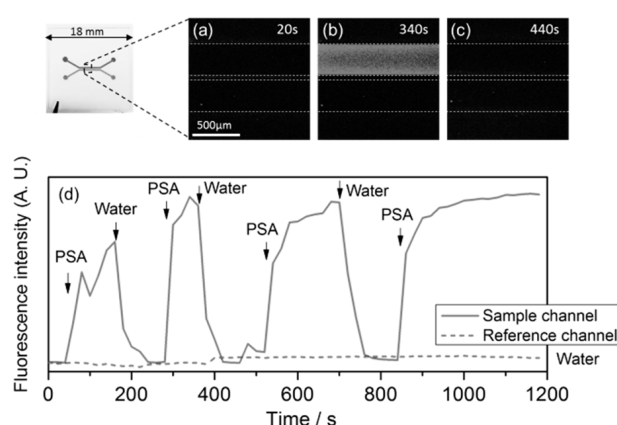


**Fig. 9.** Fluorescence images of a graphene aptasensor under microfluidic conditions observed at (a) 20, (b) 340, and (c) 440 s and (d) the average fluorescence intensities of the top and bottom channel areas over time.

tracking the fluorescence intensity at the microchannels, DI water and PSA ( $100 \mu\text{g}\cdot\text{mL}^{-1}$ ) were alternately injected in the top channel, while DI water was injected in the bottom channel throughout the measurement as a reference. Initially, both channels are filled with DI water and almost no fluorescence is observed (**Fig. 9(a)**). Clear and bright fluorescence is observed in the top channel immediately after the PSA solution is injected (**Fig. 9(b)**). **Fig. 9(d)** plots the change in the average fluorescence intensity with time. The fluorescence is repeatedly observed at similar intensity levels. This indicates that the tethered aptamer remains on the graphene surface after rinsing with DI water. This suggests that the sensor is sufficiently durable for real-time and/or continuous monitoring of target proteins under solution flow conditions.

## 9. Molecular Design for Enhanced Sensitivity

The most interesting feature of aptasensors is the ability to design and construct various kinds of biomolecular probes by incorporating additional functions with an aptamer. We can improve the sensitivity of the graphene/GO aptasensor by modifying an aptamer with an ssDNA spacer (**Fig. 10**). This increased the distance between the fluorescence dye and the graphene surface, which is crucial for FRET-based sensors [17, 18], when forming a complex with the target protein. We fabricated a  $2 \times 3$  linear-array aptasensor by using three different probes and introducing ssDNA spacers with 0, 10, and 20 thymine segments between the aptamer and the dye. The fluorescence intensity increased significantly with increases in the spacer length (**Fig. 11**). The limit for thrombin detection was about 1 nM, which corresponds to the *in vivo* concentration range during blood clotting, by using the probe with 20 thymine segments, the best design in our present study. The results show that introducing an ssDNA spacer at the correct position is an effective way of enhancing sensor sensitivity [19].

We also studied another molecular design for enhanced

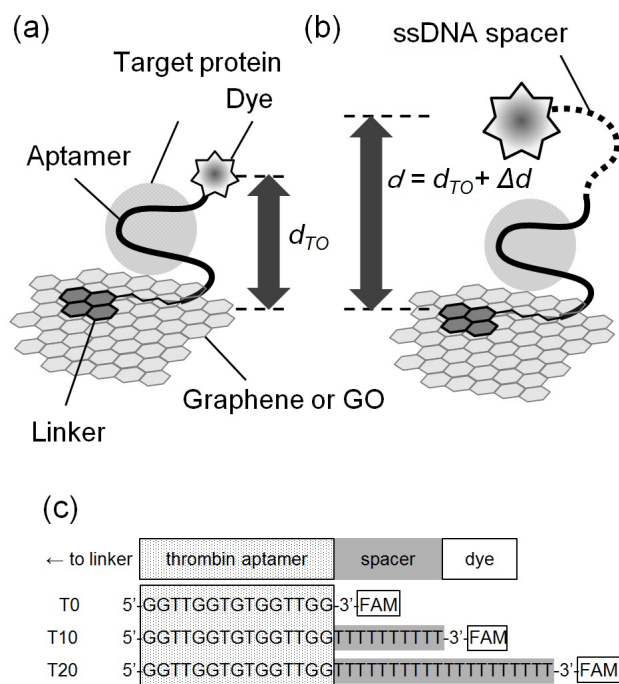
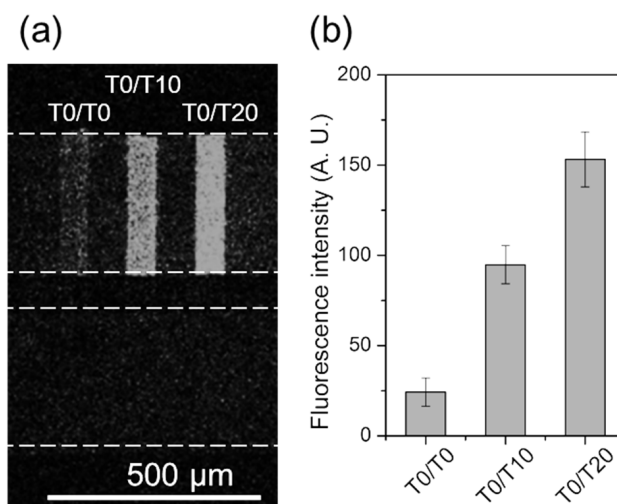


**Fig. 10.** Schematic of a technique for increasing fluorescence intensity by modifying an aptamer with a ssDNA spacer. (a) When the aptamer recognizes the target protein, the fluorescence quenching of the dye becomes less efficient as the distance between the dye and the graphene/GO surface ( $d$ ) increases. (b) The increase in ( $d$ ) becomes more potent by introducing a spacer between the aptamer sequence and the dye. (c) Design of the probes consisting of linker, thrombin aptamer, spacer, and dye. They are denoted as TN by using the numbers of thymines (N) for spacer.

sensitivity. We inserted a double-stranded DNA (dsDNA) as a spacer between a linker and an aptamer sequence to further extend the distance between the fluorescent dye and the graphene surface. Since dsDNA is a rigid polymer with a weak affinity to graphene/GO, the dsDNA can work effectively as a spacer. Moreover, the dsDNA spacer should interfere little with aptamer activity for any DNA sequence, because the structure is completely different from that of the aptamer, which is an ssDNA. We prepared modified aptamers with 10- and 30-base pair (bp) dsDNA spacers for thrombin and PSA detection by using thrombin- and PSA-binding DNA aptamers, respectively. We compared the sensitivity dependence on the dsDNA spacer length quantitatively by using a  $2 \times 2$  linear-array GO aptasensor patterned with the two different DNA probes. We performed a model calculation to estimate the effect of the spacer length on fluorescence recovery efficiency. The 30-bp spacer exhibited a signal approximately twice as large as that of the 10-bp spacer for both thrombin and PSA detection, indicating that longer dsDNA spacers have greater effects on the aptasensor sensitivity. We used a model to calculate the FRET recovery rate depending on the spacer length. The ratio of FRET recovery (30-bp/10-bp) was  $\sim 2$ , which agreed well with



Source: Chem. Commun. Vol.49 No.88 [15]

**Fig. 11.** (a) Fluorescence image of the  $2 \times 3$  multichannel linear-array aptasensor patterned with T0/T0, T0/T10, and T0/T20, from left to right. Thrombin solution (100  $\mu\text{mL}$ ) and DI water were injected into the top and bottom microchannels. (b) Average fluorescence intensity of the patterned area in the top microchannel.

the experimental results [20].

Many other possible designs exist for molecular probes that could be used to improve aptasensor performance.

#### Acknowledgements

This work was supported by JSPS KAKENHI Grant Number JP26286018.

#### References:

- [1] C. N. R. Rao and A. K. Sood, "Graphene: Synthesis, Properties, and Phenomena," 1<sup>st</sup> ed., Wiley-VCH, Weinheim, 2013.
- [2] H. C. Lee, W.-W. Liu, S.-P. Chai, A. R. Mohamed, C. W. Lai, C.-S. Khe, C. H. Voon, U. Hashim, and N. M. S. Hidayah, "Synthesis of Single-layer Graphene: A Review of Recent Development," Proc. Chem., Vol.19, pp. 916-921, 2016.
- [3] D. Li, M. B. Müller, S. Gilje, R. B. Kaner, and G. G. Wallace, "Processable aqueous dispersions of graphene nanosheets," Nature Nanotechnol., Vol.3, pp. 101-105, 2008.
- [4] T. Takami, T. Ito, and T. Ogino, "Self-Assembly of a Monolayer Graphene Oxide Film Based on Surface Modification of Substrates and its Vapor-Phase Reduction," J. Phys. Chem. C, Vol.24, pp. 9009-9017, 2004.
- [5] E. Morales-Naváez and A. Merkoçi, "Graphene oxide as an optical biosensing platform," Adv. Mater., Vol.24, pp. 3298-3308, 2012.
- [6] P. Zuo, X. J. Li, D. C. Dominguez, and B.-C. Ye, "A PDMS/paper/glass hybrid microfluidic biochip integrated with aptamer-functionalized graphene oxide nano-biosensors for one-step multiplexed pathogen detection," Lab Chip, Vol.13, pp. 3921-3928, 2013.
- [7] E. Treossi, M. Melucci, A. Liscio, M. Gazzano, P. Samori, and V. Palermo, "High-contrast visualization of graphene oxide on dye-sensitized glass, quartz and silicon by fluorescence quenching," J. Am. Chem. Soc., Vol.131, pp. 15576-15577, 2009.
- [8] L. Gao, C. Lian, Y. Zhou, L. Yan, Q. Li, C. Zhang, L. Chen, and K. Chen, "Graphene oxide-DNA based sensors," Biosensors and Bioelectronics, Vol.60, pp. 22-29, 2014.
- [9] K. Furukawa, Y. Ueno, E. Tamechika, and H. Hibino, "Protein recognition on a single graphene oxide surface fixed on a solid support," J. Mater Chem. B, Vol.1, pp. 1119-1124, 2013.

- [10] S. Klussmann, "The Aptamer Handbook: Functional Oligonucleotides and Their Applications," 1<sup>st</sup> ed., Wiley-VCH, Weinheim, 2006.
- [11] K. Furukawa, Y. Ueno, M. Takamura, and H. Hibino, "Graphene FRET Aptasensor," ACS Sensors, Vol.1, pp. 710-716, 2016.
- [12] Y. Ueno, K. Furukawa, K. Matsuo, S. Inoue, K. Hayashi, and H. Hibino, "On-chip graphene oxide aptasensor for multiple protein detection," Anal. Chim. Acta, Vol.866, pp. 1-9, 2015.
- [13] G. M. Walker and D.J. Beebe, "A passive pumping method for microfluidic devices," Lab Chip, Vol.2, pp. 131-134, 2002.
- [14] L. C. Bock, L. C. Griffin, L. A. Latham, E. H. Vermaas, and J. J. Toole, "Selection of single-stranded DNA molecules that bind and inhibit human thrombin," Nature, Vol.355, pp. 564-566, 1992.
- [15] N. Savory, K. Abe, K. Sode, and K. Ikebukuro, "Selection of DNA aptamer against prostate specific antigen using a genetic algorithm and application to sensing," Biosensors and Bioelectronics, Vol.26, pp. 1386-1390, 2010.
- [16] T. S. Misono and P. K. R. Kumar, "Selection of RNA aptamers against human influenza virus hemagglutinin using surface plasmon resonance," Anal. Biochem., Vol.342, pp. 312-317, 2005.
- [17] P.-J. J. Huang and J. Liu, "DNA-Length-Dependent Fluorescence Signaling on Graphene Oxide Surface," Small, Vol.8, pp. 977-983, 2012.
- [18] T. Hayashi, Y. Ishizaki, M. Michihata, Y. Takaya, and S. Tanama "Study on Nanoparticle Scizing Using Fluorescent Polarization Method with DNA Fluorescent Probe," Int. J. of Automation Technology, Vol.9, pp. 534-540, 2015.
- [19] Y. Ueno, K. Furukawa, K. Matsuo, S. Inoue, K. Hayashi, and H. Hibino, "Molecular design for enhanced sensitivity of a FRET aptasensor built on the graphene oxide surface," Chem. Commun., Vol.49, pp. 10346-10348, 2013.
- [20] Y. Ueno, K. Furukawa, A. Tin, and H. Hibino, "On-chip FRET Graphene Oxide Aptasensor: Quantitative Evaluation of Enhanced Sensitivity by Aptamer with a Double-stranded DNA Spacer," Anal. Sci., Vol.31, pp. 875-879, 2015.



**Name:**  
Kazuaki Furukawa

**Affiliation:**  
School of Science and Engineering, Meisei University

**Address:**  
2-1-1 Hodokubo, Hino, Tokyo 191-8506, Japan

**Brief Biographical History:**  
1988- NTT Basic Research Laboratories  
2000 Received Dr. Sci. degree (Waseda University)  
2016- Professor, Meisei University

**Main Works:**

- K. Furukawa, Y. Ueno, E. Tamechika, and H. Hibino, "Protein recognition on a single graphene oxide surface fixed on a solid support," J. Mater. Chem. B, Vol.1, pp. 1119-1124, 2013.
- K. Furukawa, Y. Ueno, M. Takamura, and H. Hibino, "Graphene FRET Aptasensor," ACS Sens., Vol.1, pp. 710-716, 2016.
- K. Furukawa, T. Teshima, and Y. Ueno, "Self-propelled ion gel at air-water interface," Sci. Rep., Vol.7, p. 9323, 2017.

**Membership in Academic Societies:**

- Japan Society of Applied Physics (JSAP)
- Physical Society of Japan (JPS)
- American Chemical Society (ACS)
- Chemical Society of Japan (CSJ)
- Japanese Research Association for Organic Electronics Materials (JOEM)



**Name:**  
Yuko Ueno

**Affiliation:**  
NTT Basic Research Laboratories

**Address:**  
3-1 Morinosato, Wakamiya, Atsugi, Kanagawa 243-0198, Japan

**Brief Biographical History:**  
1997 NTT Integrated Information & Energy Systems Laboratories  
2002 Received Dr. Sci. degree (The University of Tokyo)  
2014- NTT Basic Research Laboratories

**Main Works:**

- Y. Ueno, K. Furukawa, K. Matsuo, S. Inoue, K. Hayashi, and H. Hibino, "Molecular design for enhanced sensitivity of a FRET aptasensor built on the graphene oxide surface," Chem. Commun., Vol.49, pp. 10346-10348, 2013.
- Y. Ueno, R. Rungsawang, I. Tomita, and K. Ajito, "Quantitative Measurements of Amino Acids by Terahertz Time-Domain Transmission Spectroscopy," Anal. Chem., Vol.78, p. 5424, 2006.

**Membership in Academic Societies:**

- Chemical Society of Japan (CSJ)
- Japan Society for Analytical Chemistry (JSAC)
- Spectroscopical Society of Japan (SPSJ)
- Japan Society of Applied Physics (JSAP)
- Surface Science Society of Japan (SSSJ)
- Institute of Electronics, Information and Communication Engineers (IEICE)
- Society for Chemistry and Micro-Nano Systems (CHEMINAS)